Am J Physiol Endocrinol Metab 295: E1038–E1046, 2008.
First published September 2, 2008; doi:10.1152/ajpendo.00061.2008.

The role of GM-CSF in adipose tissue inflammation

Dong-Hoon Kim, Darleen Sandoval, Jacquelyn A. Reed, Emily K. Matter, Emeline G. Tolod, Stephen C. Woods, and Randy J. Seeley

Department of Psychiatry, University of Cincinnati, Cincinnati, Ohio

Submitted 30 January 2008; accepted in final form 25 August 2008

Kim DH, Sandoval D, Reed JA, Matter EK, Tolod EG, Woods SC, Seeley RJ. The role of GM-CSF in adipose tissue inflammation. *Am J Physiol Endocrinol Metab* 295: E1038–E1046, 2008. First published September 2, 2008; doi:10.1152/ajpendo.00061.2008.— Granulocyte-macrophage colony-stimulating factor (GM-CSF) is a proinflammatory cytokine that has a central action to reduce food intake and body weight. Consistent with this, GM-CSF knockout mice are more obese and hyperphagic than wild-type mice. However, in lung, GM-CSF is an important determinant of macrophage infiltration. Consequently, we sought to determine if GM-CSF might contribute to adipose tissue macrophage accumulation, insulin resistance, and low-grade inflammation that occurs when animals gain weight on a high-fat diet (HFD). We therefore determined how targeted genetic disruption of GM-CSF can affect adipose tissue macrophage and cytokine gene expression as well as glucose homeostasis by performing hyperinsulinemic-euglycemic clamps. The number of macrophages and CCR2 gene expression in adipose tissue of GM-CSF knockout mice was decreased relative to those in wild-type mice, and the adipocyte size of mesenteric fat was increased in GM-CSF knockout mice on a HFD compared with wild-type mice. The level of mRNA of the proinflammatory cytokines interleukin-1β, tumor necrosis factor-α, and macrophage inflammatory protein-1α was significantly lower in mesenteric fat of GM-CSF knockout mice on the HFD than in wild-type mice. Using the hyperinsulinemic-euglycemic clamp technique, GM-CSF knockout mice had greater overall insulin sensitivity. This increase was due to enhanced peripheral uptake and utilization of glucose rather than to increased hepatic insulin sensitivity. Collectively, the data suggest that the GM-CSF knockout mutation ameliorates peripheral insulin resistance in spite of increased adiposity by reducing inflammation in adipose tissue in response to a HFD.

granulocyte-macrophage stimulating factor; adipose tissue inflammation; insulin resistance; macrophage; hyperinsulinemic-euglycemic clamp

GRANULOCYTE-MACROPHAGE colony-stimulating factor (GM-CSF) is a proinflammatory cytokine that induces myeloid-lineage differentiation of hematopoietic stem cells (7, 9). It also promotes maturation and other cell functions of myeloid-lineage cells, particularly those of granulocytes and macrophages (18, 35). GM-CSF is a potent chemotactic factor for macrophages and other immune cells and induces expression of cell adhesion molecules, including CD11a and CD11c (21). GM-CSF also upregulates tumor necrosis factor (TNF)-α and interleukin (IL)-1β gene expression and is further induced by TNF-α and IL-1β in immune cells infiltrating a site of inflammation (11, 27, 31).

In previous studies, we found that GM-CSF receptors are found on key hypothalamic neurons. Central (but not peripheral) injection of a single dose of GM-CSF in the third cerebral ventricle decreased food intake and body weight in rats and mice without causing illness. Mice with targeted genetic disruption of the GM-CSF locus had increased body weight with two- to threefold increases in adipose mass (24). Taken together, these data indicate an important role for GM-CSF in the central nervous system (CNS) regulation of food intake and body fat.

Obesity in humans and rodents has been linked to inflammation in visceral adipose tissue, accompanied by accumulation of adipose tissue macrophages (34, 37). This inflammation is characterized by increased expression of proinflammatory cytokines, including TNF-α, IL-1β, IL-6, and macrophage inflammatory protein (MIP)-1α in total adipose tissue. Adipocytes and activated macrophages contribute to the expression of these cytokines (28), and they are hypothesized to contribute to obesity-induced insulin resistance as well (29, 37).

In the present study, we evaluated a possible role of GM-CSF in adipose tissue inflammation. Because overexpression of GM-CSF has resulted in accumulation of macrophages in several transgenic models (12, 13), we sought to identify whether loss of GM-CSF signaling decreases adipose tissue macrophage numbers and adipose tissue inflammation, particularly in response to a high-fat diet (HFD). We also used euglycemic-hyperinsulinemic clamps to assess any resulting changes in peripheral insulin sensitivity.

MATERIALS AND METHODS

Animals

GM-CSF knockout mice on a C57Bl/6 background were described previously (24). Wild-type C57Bl/6 mice were obtained from Jackson Laboratories. Beginning at 8 wk of age, male mice were housed individually in standard mouse cages with a 12:12-h light-dark cycle. They had ad libitum access to either a HFD providing 40% calories as fat (D03082706; Research Diets) or a low-fat diet (LFD) with 10% fat (D03082705) for 12 wk, as previously described (36). The two sets of experiments using the LFD and HFD were performed on different cohorts of animals. All animal protocols were approved by the University of Cincinnati Institutional Animal Care and Use Committee.

Counting Macrophages

To determine macrophage accumulation in mesenteric fat, we used a method adapted from Weisberg et al. (34). Briefly, adipose tissue was formalin-fixed, and adipose tissues were postfixed overnight and processed for paraffin embedding. Tissue was sectioned at 4 μm. Slides were deparaffinized and boiled for 15 min in citrate buffer, pH 6.0. Sections were blocked with 0.1% normal goat serum (NGS) in PBS-Tween 20 (PBS-T) for 1 h and incubated overnight at 4°C in anti-F4/80 (Caltag Laboratories, Burlingame, CA) diluted 1:1,000 in 0.1% NGS in PBS-T. On *day 2*, slides were rinsed and

Address for reprint requests and other correspondence: R. J. Seeley, 2170 East Galbraith Rd., E-312, Cincinnati, OH 45237 (e-mail: randy.seeley@uc.edu).

The costs of publication of this article were defrayed in part by the payment of page charges. The article must therefore be hereby marked "*advertisement*" in accordance with 18 U.S.C. Section 1734 solely to indicate this fact.

incubated in biotinylated anti-rat (Jackson ImmunoResearch Laboratories, West Grove, PA) diluted 1:250 in 0.1% NGS for 1 h, incubated in the ABC Vectastain System (Vector Laboratories, Burlingame, CA), and then incubated for 30 min in fluorescein isothiocyanate-conjugated streptavidin (Jackson ImmunoResearch Laboratories). Slides were rinsed and coverslipped with Vectashield with 4′,6-diamidino-2-phenylindole (DAPI; Vector Laboratories). Immunofluorescence reactivity or DAPI was detected by confocal microscopy (LSM 510 Meta; Zeiss). Relative numbers of macrophages were determined by dividing macrophage count per 100 nuclei in consecutive high-power fields overlaid with a grid with numbered areas. Counts were performed in triplicate by blinded observers using a different section for each count and counting in grid areas as assigned by a random number generator.

Adipocyte Tissue Morphometry

To determine adipocyte size, the cross-sectional area of adipocytes was measured on paraffin-embedded hematoxylin- and eosin-stained sections of mesenteric fat at a magnification of ×200 by image processing with ImageJ 1.40g software (National Institutes of Health, Bethesda, MD). The way of determining adipocyte size was modified using a computer image analysis (2). Briefly, after converting the image of adipose tissue to a binary image, each adipocyte was manually delineated by the command of Paintbrush to ensure an accurate contour of adipose tissue. The cross-sectional area of adipocytes was calculated with the command of Analyze Particle of ImageJ, and the results were analyzed by a spreadsheet program (Microsoft Excel 2003; Microsoft, Redmond, WA). The distribution of adipocyte size was determined by relative frequencies of adipocytes having a size within a regular interval. The mean adipocyte area was determined by dividing the sum of adipocyte areas by the number of adipocytes. The number of crown-like structures (CLS) was counted on the hematoxylin- and eosin-stained sections and divided by the number of adipocytes (200~500). The density of CLS was expressed as CLS per 100 adipocytes (4, 30).

Adipose Proinflammatory Cytokine Gene Expression

As previously described (24), mice were killed during the phase after a 4-h fast. The mesenteric, epididymal, and inguinal fat pads were quickly removed and stored in RNA/later (Ambion). Total RNA was isolated, and cDNA was synthesized using iScript (Bio-Rad) and verified by L32 amplification products in agarose gel. All RT-PCR were performed using Failsafe PCR kits (EPICENTRE Biotechnologies, Madison, WI). Mouse Q-PCR primer sequences are as follows: *L32,* forward primer 5′-GCCAGGAGACGACAAAAAT and reverse primer 5′-AATCCTCTTGCCCTGATCC at 61.2°C; *GM-CSF*, forward primer 5′-ACCACCTATGCGGATTTCAT and reverse primer 5′-TCATTACGCAGGCACAAAAG at 61.2°C; monocyte chemoattractant protein (*MCP*)*-1,* forward primer 5′-CCCAATGAGTAGGCTGGAGA and reverse primer 5′-TCTGGACCCATTCCTTCTTG at 61.2°C; *CCR2,* forward primer 5′-ACACCCTGTTTCGCTGTAGG and reverse primer 5′-GATTCCTGGAAGGTGGTCAA at 61.2°C; *TNF-α,* forward primer 5′-CCCCAAAGGGATGAGAAGTT and reverse primer 5′-CACTTGGTGGTTTGCTACGA at 61.2°C; *IL-1β*, forward primer 5′-GGGCTGCTTCCAAACCTTTG and reverse primer 5′-TGATACTGCCTGCCTGAAGCTC at 61.2°C; *MIP-1α*, forward primer 5′-CAGCCAGGTGTCATTTTCCT and reverse primer 5′-CTGCCTCCAAGACTCTCAGG at 61.2°C; *CD68*, forward primer 5′-TTCTGCTGTGGAAATGCAAG and reverse primer 5′-AGAGGGGCTGGTAGGTTGAT at 64.3°C. Each primer set was optimized such that the correlation was 0.99–1.0 and the PCR efficiency was 90–100%. PCR was performed in triplicate using an iCycler and the iQ SYBR Green Supermix (Bio-Rad Laboratories) with two-step amplification (95°C for 10 s, annealing temperature for 30 s) for 40 cycles. L32 was amplified from every sample for use as an endogenous control. For the data analysis, the average threshold cycle (C_T) of each set of triplicates was calculated. To normalize the data, the ΔC_T was calculated for each sample by subtracting the average C_T of L32 from the average C_T of the gene of interest. For relative quantitation, the ΔC_T was averaged for the defined control group and was then subtracted from the ΔC_T of each experimental sample to generate the $\Delta\Delta C_T$. The $\Delta\Delta C_T$ was then used to calculate the approximate fold difference, $2^{\Delta\Delta CT}$ (Applied Biosystem's instructions) (6, 24).

Hyperinsulinemic-Euglycemic Clamp

C57Bl/6 and GM-CSF knockout mouse strains were backcrossed for two generations and genotyped to identify GM-CSF knockouts and wild-type controls. Male wild-type or GM-CSF knockout mice were maintained individually in microisolator cages and fed a HFD providing 40% calories as fat (D03082706; Research Diet) ad libitum beginning at 12 wk of age. All procedures performed for the clamp experiments were conducted at the Vanderbilt Mouse Metabolic Phenotyping Center and were preapproved by the Vanderbilt University Animal Care and Use Subcommittee. Insulin experiments were performed on mature mice (~5–6 mo of age), since the larger size of these mice facilitated implantation of the carotid artery catheter. Mice were anesthetized with a mixture of rompun and ketamine (~2 and 2.5 mg/mouse, respectively). The left common carotid artery was catheterized with a two-part catheter consisting of PE-10 tubing (portion inserted in artery) and a Silastic catheter [0.025 in outer diameter (OD)]. The right jugular vein was catheterized with a one-part Silastic catheter (0.025 in OD). The free ends of catheters were tunneled under the skin to the back of the neck, where they were attached via stainless steel connectors to lines made of Micro-Renathane (0.033 in OD), which were exteriorized and sealed with stainless steel plugs. Lines were cleared daily with saline containing 200 U/ml of heparin and 5 mg/ml of ampicillin. Body weight was monitored daily, and animals were used for experiments once they were within 2 g of presurgery body weight (~5 days). Animals were housed individually after surgery.

On the day of the study, conscious 5-h fasted mice were placed in 2,000-ml plastic beakers, and Micro-Renathane (0.033 in OD) tubing was connected to infusion syringes and catheter leads. After the mice adapted to their surroundings (~30 min), a baseline sample was drawn for measurement of hematocrit, glucose, and insulin. A 5-μCi bolus of [3-^{3}H]glucose was given at time (t) = 90 min before insulin infusion, followed by a 0.05 μCi/min infusion for 90 min. An insulin infusion rate of 4 $mU \cdot kg^{-1} \cdot min^{-1}$ (n = 8 wild type and n = 12 knockout) was started (t = 0 min), and glucose (50 g/100 ml) was infused as necessary to maintain euglycemia on the basis of feedback from frequent arterial glucose measurements (~5 μl; HemoCue, Mission Viejo, CA). The [3-^{3}H]glucose infusion was increased to 0.2 μCi/min for the remainder of the experiment. A 12-μCi bolus of 2-[^{14}C]deoxyglucose (2[^{14}C]DG) was given at t = 78 min. Blood samples (80–240 μl) were taken every 10 min from t = 80–120 min and processed to determine plasma [3-^{3}H]glucose and 2[^{14}C]DG. Previous results have demonstrated that the blood volume taken during these experiments (~400 μl) results in a minimal fall in hematocrit (~5%) (10).

Analytical methods. Immunoreactive insulin was measured with a double-antibody method (10). Plasma was deproteinized with barium hydroxide [$Ba(OH)_2$, 0.3 N] and zinc sulfate ($ZnSO_4$, 0.3 N), and 2[^{3}H]DG radioactivity was then determined by liquid scintillation counting (Beckman LS 5000TD; Beckman Instruments) with Ecolite+ as the scintillant. Muscle samples were weighed and homogenized in 0.5% perchloric acid. Homogenates were centrifuged and neutralized with KOH. One aliquot was counted directly to determine 2[^{14}C]DG and 2[^{14}C]DG-6-phosphate (2[^{14}C]DGP) radioactivity. A second aliquot was treated with $Ba(OH)_2$ and $ZnSO_4$ to remove 2[^{14}C]DGP and any tracer incorporated into glycogen and then counted to determine 2[^{14}C]DG radioactivity. 2[^{14}C]DGP is the difference be-

tween the two aliquots. In all experiments, the accumulation of 2[^{14}C]DGP was normalized to tissue weight.

Tracer calculations. Rates of glucose appearance (R_a), hepatic glucose production, and glucose utilization were calculated according to the methods of Wall et al. (32) and as described previously (26). Briefly, endogenous glucose production was calculated by determining the total R_a (this comprises both hepatic glucose production and any exogenous glucose infused to maintain the desired glycemic levels) and subtracting it from the amount of exogenous glucose infused. Glycolytic rates were estimated from the increment per unit time of ^3H_2O multiplied by the estimated body water divided by [3-^{3}H]glucose specific activity. ^3H_2O appearance was determined by linear regression of the measures at $t = 80–120$ min. Body water was assumed to be 60% of body weight (5).

Statistical Analyses

Differences between groups were determined with Student's *t*-test. A P value <0.05 was considered statistically significant.

RESULTS

The Number of Macrophages Was Decreased in White Adipose Tissue of GM-CSF Knockout Mice on a HFD Relative to Those in Wild-Type Mice

Body weight of GM-CSF knockout mice on the HFD was 31.00 ± 1.58 and that of wild-type mice was 26.78 ± 0.89 (see Fig. 2*D*). To determine a role of GM-CSF in recruiting macrophages, we counted the number of macrophages in mesenteric fat of wild-type mice and GM-CSF knockout mice on the HFD by staining with anti-F4/80 antibody, where GM-CSF was most highly expressed, compared with epididymal or subcutaneous fat [Supplemental Fig. 1 (Supplementary data for this article can be found at the *American Journal of Physiology: Endocrinology and Metabolism* web site.)]. The number of macrophages in mesenteric fat of GM-CSF knockout mice

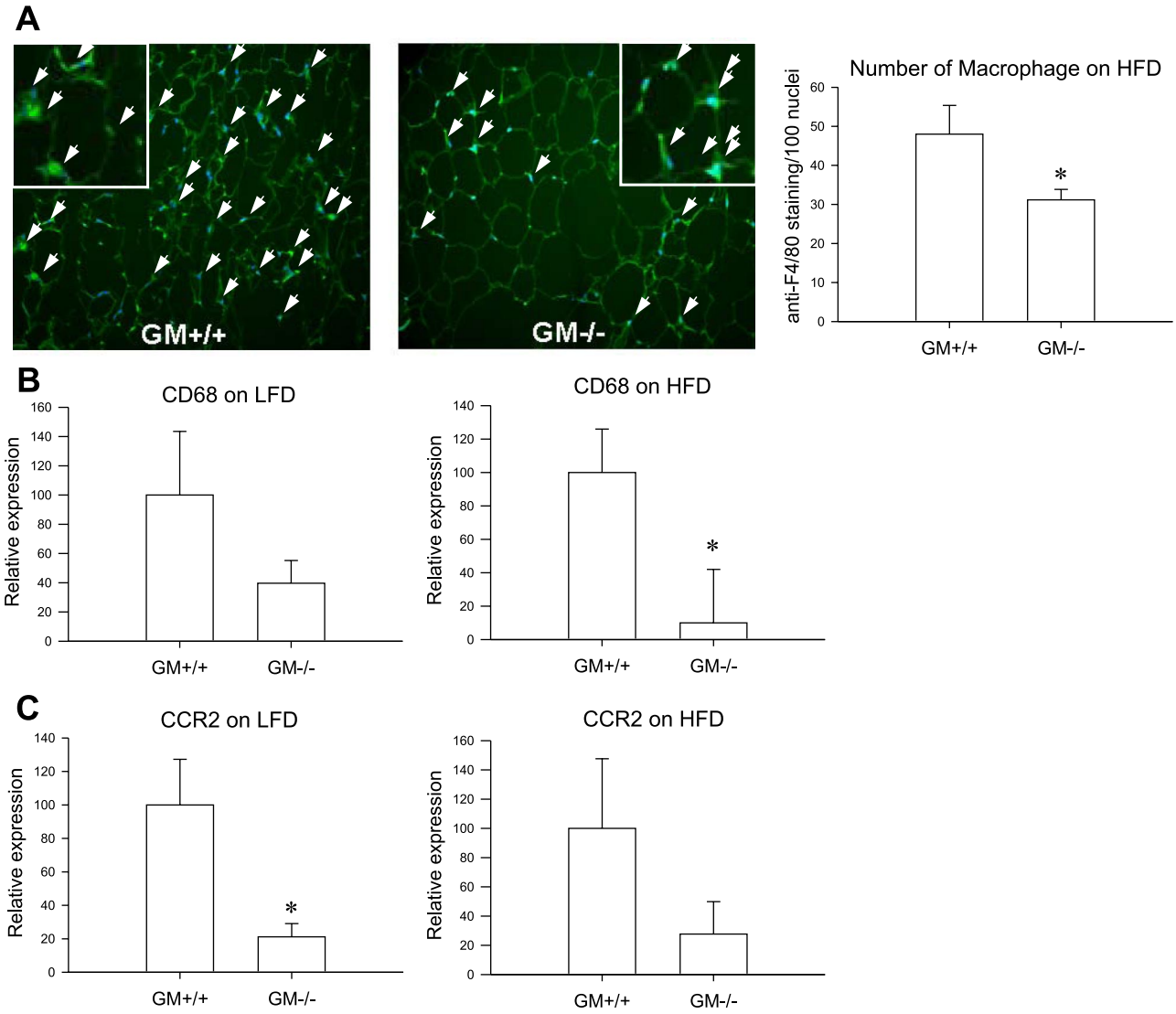

Fig. 1. Representative figures of anti-F4/80 staining in mesenteric fat of wild-type mice and granulocyte-macrophage colony-stimulating factor (GM-CSF) knockout mice on a high-fat diet (HFD). White arrows indicate colocalization of F4/80 staining and 4′,6-diamidino-2-phenylindole (DAPI). No. of macrophages was determined by counting anti-F4/80 staining (bright green) per 100 nuclei (blue) in *A*. *B*: CD68 mRNA expression in mesenteric fat of wild-type mice ($n = 6$) and GM-CSF knockout mice ($n = 4$). *C*: CCR2 mRNA expression in mesenteric fat of wild-type mice and GM-CSF knockout mice on a low-fat diet ($n = 7$ and $n = 8$) or HFD ($n = 6$ and $n = 5$, respectively). *$P < 0.05$, wild-type mice vs. GM-CSF knockout mice.

was significantly lower than that in wild-type mice on the HFD ($P < 0.05$, 31.17 ± 2.68 vs. 48.01 ± 7.33; Fig. 1*A*). Consistently, CD68 gene expression was also significantly lower in mesenteric fat of GM-CSF knockout mice on the HFD ($P < 0.05$; Fig. 1B), and the formation of CLS was reduced in mesenteric fat of GM-CSF knockout mice (1.13 ± 0.37/100 adipocytes) compared with wild-type mice (8.33 ± 1.40/100 adipocytes; $P < 0.001$) (Fig. 2*A*). Because CD68 expression is a marker of macrophages, this finding suggests that GM-CSF expression correlates with the relative number of macrophages.

To determine whether a deficiency in GM-CSF affects adipocyte morphology, we compared the adipocyte size in mesenteric fat of wild-type and GM-CSF knockout mice on the HFD. The mean adipocyte size of GM-CSF knockout mice was significantly higher than that of wild-type mice (Fig. 2, *B* and *C*), which stands in contrast to previous findings that correlated adipocyte size with the number of macrophages in adipose tissue (34).

To investigate whether the decrease in number of macrophages was involved in CCR2 signaling (33), we evaluated the level of CCR2 and MCP-1 mRNA expression in wild-type and GM-CSF knockout mice on the LFD and HFD. CCR2 mRNA expression was significantly lower in mesenteric fat of knockout mice than in wild-type mice on the LFD ($P < 0.05$, 1.00 ± 0.27 vs. 0.21 ± 0.08), but this did not reach statistical significance in mice maintained on the HFD (Fig. 1*C*). However, there was no difference in MCP1 mRNA expression in mesenteric fat of GM-CSF knockout mice on the LFD vs. those maintained on the HFD (data not shown).

Proinflammatory Cytokines in Mesenteric Fat of GM-CSF Knockout Mice

We compared the levels of mRNA expression of proinflammatory cytokines in mesenteric fat of wild-type mice on the HFD with those of GM-CSF knockout mice. While on a LFD,

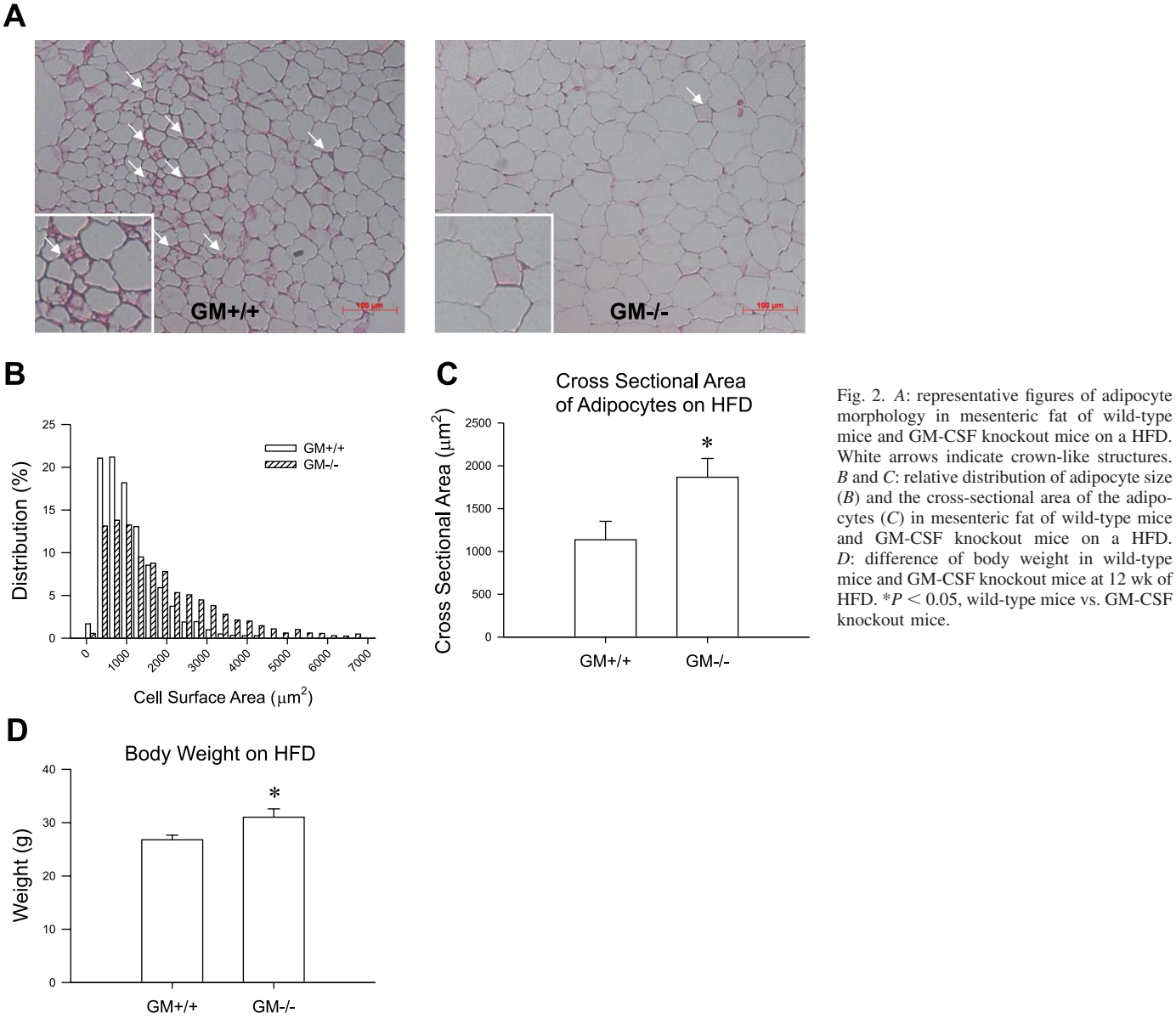

Fig. 2. *A*: representative figures of adipocyte morphology in mesenteric fat of wild-type mice and GM-CSF knockout mice on a HFD. White arrows indicate crown-like structures. *B* and *C*: relative distribution of adipocyte size (*B*) and the cross-sectional area of the adipocytes (*C*) in mesenteric fat of wild-type mice and GM-CSF knockout mice on a HFD. *D*: difference of body weight in wild-type mice and GM-CSF knockout mice at 12 wk of HFD. *$P < 0.05$, wild-type mice vs. GM-CSF knockout mice.

there were only nonsignificant trends for lower expression of IL-1β, TNF-α, and MIP-1α mRNA in GM-CSF knockouts (Fig. 3*A*). However, when the GM-CSF knockouts were placed on a HFD, relative expression of all three cytokines was significantly reduced compared with wild-type control mice on the same diet (Fig. 3*B*).

Glucose Homeostasis in GM-CSF Knockout Mice

Hyperinsulinemic-euglycemic clamp. Glucose levels during the clamp (144 ± 13 vs.143 ± 7) did not change significantly from baseline (158 ± 18 vs. 149 ± 6) in either group (GM-CSF knockout mice vs. wild-type mice). However, insulin levels were significantly lower at baseline and consequently also during the clamp in GM-CSF knockout mice than in wild-type mice (Fig. 4*A*). Despite the lower insulin levels, the exogenous glucose infusion required to maintain similar glucose levels during the clamp tended ($P = 0.07$) to be greater in GM-CSF knockout mice than in wild-type mice (Fig. 4*B*). When expressed relative to insulin levels (Fig. 4*G*), the glucose infusion rate was significantly greater in GM knockout mice than in wild-type mice, indicating greater whole body insulin sensitivity. Isotope dilution techniques indicated that this was the result of an overall greater glucose clearance during basal and clamp periods in GM-CSF knockout mice than in wild-type mice (Fig. 4*C*). While endogenous glucose production was also greater in the GM-CSF knockout mice at baseline and during the clamp (Fig. 4*D*), percent inhibition of endogenous glucose production was similar between the groups (34 ± 11 vs. 46 ± 15% in GM-CSF knockout mice vs. wild-type mice, respectively). The increase in glucose clearance was due to an increase in glucose utilization rather than storage (Fig. 4*E*), as indicated by a greater whole body rate of glycolysis (Fig. 4*F*). Using tritiated 2-deoxyglucose, we found that absolute glucose uptake was similar between the groups across a number of tissues (Table 1). When expressed relative to insulin levels, glucose uptake was greater in the vastus, diaphragm, heart, and brain (Table 1). Thus these data indicate that a deficiency in GM-CSF leads to changes in glucose metabolism at both the level of the liver and skeletal muscle and that these changes result in improved overall glucose tolerance despite increased body fat.

DISCUSSION

The aim of this study was to determine whether GM-CSF plays a significant role in adipose tissue inflammation by recruiting and activating macrophages in adipose tissue. In previous studies, we found that GM-CSF has a central action

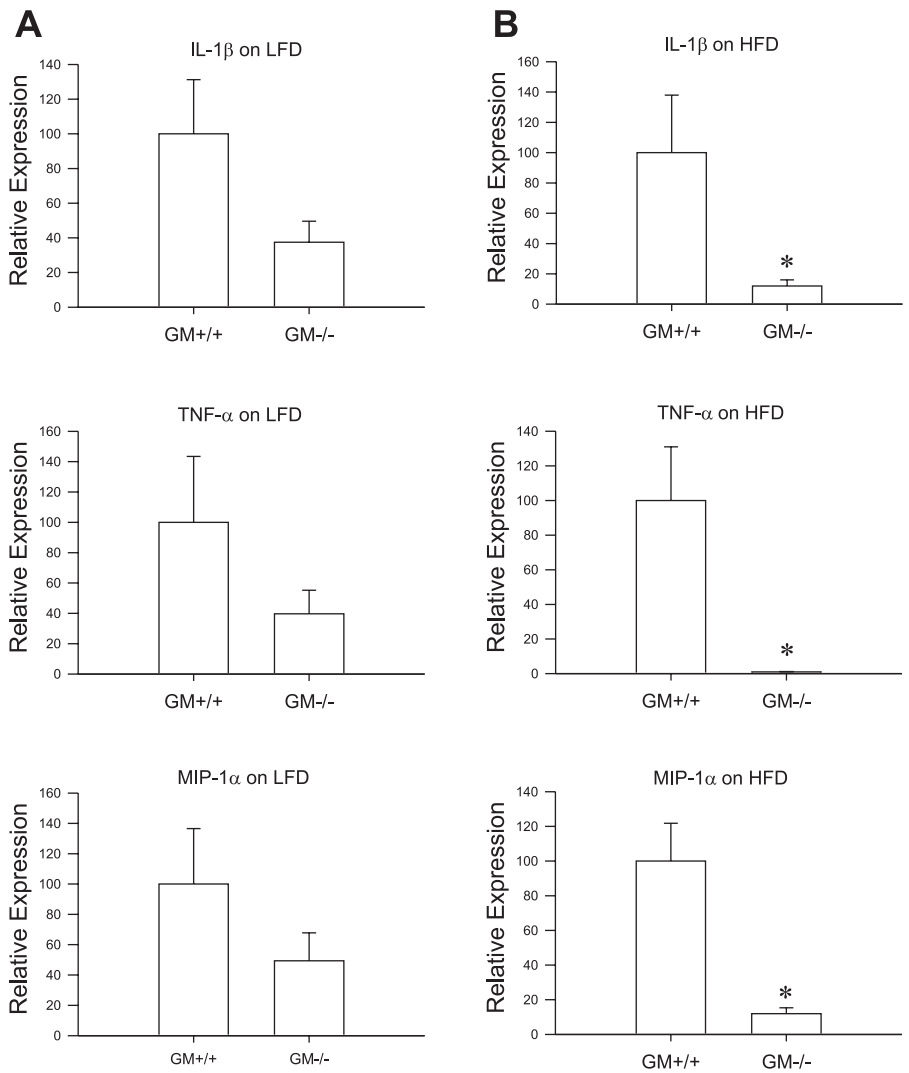

Fig. 3. Proinflammatory cytokine mRNA expression in mesenteric fat of wild-type mice and GM-CSF knockout mice on a low-fat diet ($n = 7$ and $n = 8$; *A*) or HFD ($n = 6$ and $n = 4$, respectively; *B*). *$P < 0.05$, wild-type mice vs. GM-CSF knockout mice.

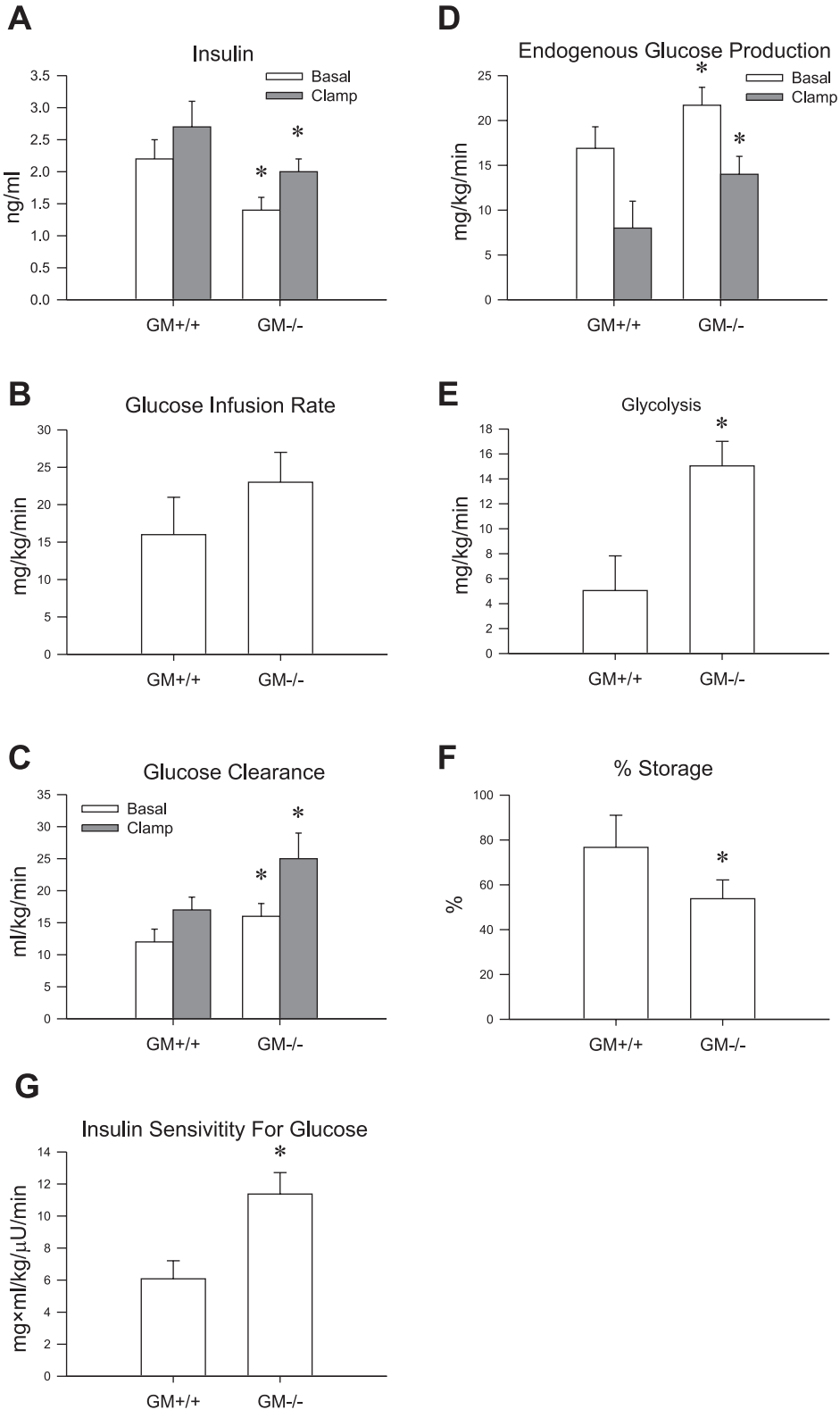

Fig. 4. Hyperinsulinemic-euglycemic clamp was performed in 5-h-fasted wild-type ($n = 8$) and GM-CSF knockout mice ($n = 12$) on a HFD. *A*: basal and clamp insulin levels. *B*: glucose infusion rate during the final 30 min of the clamp. *C*: glucose clearance during the final 30 min of the clamp. Glucose clearance was significantly greater at baseline and during the end of the clamp in the GM-CSF knockout mice. *D*: endogenous glucose production at baseline and during the last 30 min of the 2-h clamp was significantly greater in GM-CSF knockout mice. *E* and *F*: glycolytic rate was significantly greater (*E*) and glucose storage was significantly lower (*F*) at the end of the clamp in GM-CSF knockout mice. *G*: insulin sensitivity to glucose calculated via the glucose infusion rate (GIR) divided by insulin levels was significantly greater in GM-CSF knockout mice. *$P < 0.05$, wild-type mice vs. GM-CSF knockout mice.

on food intake and that a deficiency of GM-CSF causes greater adiposity and increased food intake (24), but we hypothesized that GM-CSF would also act as a chemokine for immune cells in the periphery. Consistent with this hypothesis, we found that GM-CSF expression is different across different fat pads, with the highest expression in mesenteric fat (Supplementary Fig. 1). Importantly, we also found that, despite greater body fat, the adipose tissue of GM-CSF knockout mice had fewer macrophage markers, and on a HFD the knockouts had reduced expression of proinflammatory cytokines.

Table 1. *Absolute and relative to insulin levels of tissue glucose uptake in various tissues*

	$GM^{+/+}$	$GM^{-/-}$
Rg, $\mu mol \cdot 100\ g\ tissue^{-1} \cdot min^{-1}$		
Soleus	40±10	32±9
Gastricnemius	7±1	7±1
Vastus	5±1	6±1
Diaphragm	73±13	120±16*
Heart	210±42	253±43
Brain	33±5	41±4
Adipose	1.7±0.4	1.8±0.5
Rg/insulin, $\mu mol \cdot ml \cdot 100\ g\ tissue^{-1} \cdot \mu U^{-1} \cdot min^{-1}$		
Soleus	15±4	16±5
Gastrocnemius	2.7±0.4	3.6±0.7
Vastus	1.9±0.4	3.0±0.5*
Diaphragm	28±5	60±8*
Heart	79±16	125±21*
Brain	12±2	20±2*
Adipose	0.6±0.1	0.9±0.3

Values are means ± SE. GM, granulocyte-macrophage colony-stimulating factor (GM-CSF) sufficient (+/+) and deficient (−/−); Rg, tissue-specific index of glucose uptake. *$P < 0.05$, wild-type mice vs. GM-CSF knockout mice.

As its name indicates, GM-CSF also plays a role as a hematopoietic growth factor, stimulating stem cells to produce granulocytes as well as monocytes. A number of studies have reported that GM-CSF can act as a strong chemoattractant for monocytes and is a macrophage maturation and activation factor in the lung (19, 25, 39), with GM-CSF knockout mice having lower tissue macrophage populations in the lung (21, 25, 39). The present results extend this to adipose tissue. Given the lower level of macrophages in the mesenteric fat of GM-CSF knockouts, the fat depot where GM-CSF expression is the highest in wild-type mice, it would appear that GM-CSF plays a similar role in adipose tissue, either as a recruitment or activation factor, or both. Another issue is the larger adipocyte size with lower macrophage number in adipose tissue of GM-CSF knockout mice. Previous work has indicated that the size of adipocytes is proportional to the number of macrophages (34), and it was suggested that the macrophage plays a role in adipose tissue remodeling by scavenging dead adipocytes (4, 30). The current data indicate that increased adipocyte size is not sufficient to drive increased macrophage infiltration. One possibility is that GM-CSF is simply necessary for macrophage recruitment in response to adipocyte death. Another possibility is that GM-CSF plays a role in inhibiting adipocyte hypertrophy or adipogenesis, making the existing adipocytes more stable. Limited adipocyte death would then lower the resulting macrophage infiltration, since there would be no need to solubilize the lipid droplets left behind after the adipocyte dies.

Recruited macrophages stimulated by interferon-γ, lipopolysaccharide, or TNF-α have high bacteriocidal activity and inflammatory response and are called M1 or "classically activated" macrophages (8, 16, 17). In contrast, resident macrophages stimulated in vitro by IL-4, IL-13, or transforming growth factor-β reflect activity of tissue repair and suppress inflammation and are called M2 or "alternatively activated" macrophages (8, 16, 17). Recently, it was reported that inflammation is aggravated when alternatively activated macrophages are reduced in adipose tissue of macrophage-specific peroxisome proliferator-activated receptor-γ knockout mice (20). A key issue in adipose tissue biology is whether adipose tissue macrophages lead to higher levels of inflammation under different circumstances, and our hypothesis is that GM-CSF would work to recruit and activate M1 macrophages and thus contribute to adipose tissue inflammation. The current data indicate that GM-CSF also plays a role in this increased expression of proinflammatory cytokines as well. Despite the significant increases in body adiposity observed in GM-CSF knockout animals on a HFD (24), the expressions of IL-1β, TNF-α, and MIP-1α are lower in the GM-CSF knockout mice compared with their leaner wild-type controls. Such data indicate that GM-CSF also contributes to adipose tissue inflammation, since it acts as a chemoattractant for monocytes and activator for macrophages. On the other hand, GM-CSF may play a role in normal function of macrophages as a maturation factor in adipose tissue, as seen in lung where GM-CSF is involved in critical functions of macrophages such as pulmonary surfactant metabolism and responses to bacterial microorganisms that protect the lungs from infection (15, 22, 25, 38, 39). Therefore, it would be possible that "immature" macrophages may contribute to the impaired production of proinflammatory cytokines in adipose tissue of GM-CSF knockout mice.

One hypothesis about the link between obesity and type II diabetes is that increased inflammation and cytokine secretion from adipose tissue leads to insulin resistance, particularly in the liver (3, 23, 29). Based on this hypothesis, it would be predicted that, since the GM-CSF knockouts had reduced expression of at least three different cytokines, hepatic insulin sensitivity would be greater in the knockouts vs. the wild-type mice. Our data do not support this prediction. Absolute glucose production was greater in the knockout mice under basal and clamp conditions, which at a first pass would suggest impaired rather than improved hepatic insulin sensitivity. However, insulin levels were lower under basal and clamp conditions in the knockout mice, and this would increase glucose production independently of hepatic insulin resistance. In fact, both groups of mice clearly had some degree of hepatic insulin resistance on the HFD, since the suppression of glucose production during the clamp was 34 and 46% in knockout and wild-type mice, respectively, compared with 90% in C57Bl/6J mice on a LFD (1). Thus lack of the GM-CSF gene and the reduced adipose tissue expression of TNF-α, IL-1β, and MIP-1α did not have a protective effect on hepatic insulin sensitivity.

It is interesting that the GM-CSF knockout mice did have some degree of protection from peripheral insulin insensitivity caused by the HFD relative to wild-type mice. This is illustrated by the fact that, despite the lower insulin levels, and increased glucose production, glucose levels were maintained similar to those of wild-type mice, likely because of significantly increased glucose clearance during both basal and clamp conditions in the knockouts vs. the wild-type mice. Similarly, when the exogenous glucose infusion rate and tissue glucose uptake were expressed relative to insulin levels (insulin sensitivity to glucose), the data supported the conclusion that whole body insulin sensitivity was greater in GM-CSF knockout mice than wild-type mice. Furthermore, tissue glucose uptake expressed relative to insulin levels was significantly higher in the vastus and other highly oxidative muscles (diaphragm, heart)

of GM-CSF knockout mice compared with wild-type controls. In summary, peripheral but not hepatic insulin sensitivity was preserved with knock out of the GM-CSF gene. However, taken together, these results do not easily support the hypothesis that visceral fat adipose tissue cytokine secretion is a primary effector of liver insulin resistance, at least in the context of GM-CSF deficiency.

The existing data on GM-CSF emphasize two distinct metabolic effects. One is the ability of GM-CSF acting in the CNS to regulate food intake and body adiposity. That effect appears to be the result of actions on GM-CSF receptors in key hypothalamic nuclei and the ability to activate STAT5 signaling (14). The current data, however, argue that GM-CSF also plays an important role in adipose tissue to recruit and activate macrophages. Moreover, it would also appear to play an important role in overall levels of proinflammatory cytokine expression in adipose tissue, particularly when mice are maintained on a HFD.

ACKNOWLEDGMENTS

We thank the Vanderbilt MMPC (DK-59637) for providing the hyperinsulinemic-euglycemic clamp data in the wild-type and GM-CSF knockout mice. We also thank Troy Hibbard for preparing adipose tissue sections for histological study.

GRANTS

This work was supported by National Institute of Diabetes and Digestive and Kidney Diseases Grants DK-073505 and DK-056863.

REFERENCES

1. **Ayala JE, Bracy DP, McGuinness OP, Wasserman DH.** Considerations in the design of hyperinsulinemic-euglycemic clamps in the conscious mouse. *Diabetes* 55: 390–397, 2006.
2. **Bjornheden T, Jakubowicz B, Levin M, Oden B, Eden S, Sjostrom L, Lonn M.** Computerized determination of adipocyte size. *Obes Res* 12: 95–105, 2004.
3. **Bjorntorp P.** Regional fat distribution–implications for type II diabetes. *Int J Obes Relat Metab Disord* 16, *Suppl* 4: S19–S27, 1992.
4. **Cinti S, Mitchell G, Barbatelli G, Murano I, Ceresi E, Faloia E, Wang S, Fortier M, Greenberg AS, Obin MS.** Adipocyte death defines macrophage localization and function in adipose tissue of obese mice and humans. *J Lipid Res* 46: 2347–2355, 2005.
5. **Clodi M, Thomaseth K, Pacini G, Hermann K, Kautzky-Willer A, Waldhusl W, Prager R, Ludvik B.** Distribution and kinetics of amylin in humans. *Am J Physiol Endocrinol Metab* 274: E903–E908, 1998.
6. **Cota D, Proulx K, Smith KA, Kozma SC, Thomas G, Woods SC, Seeley RJ.** Hypothalamic mTOR signaling regulates food intake. *Science* 312: 927–930, 2006.
7. **Dranoff G, Crawford AD, Sadelain M, Ream B, Rashid A, Bronson RT, Dickersin GR, Bachurski CJ, Mark EL, Whitsett JA, Mulligan RC.** Involvement of granulocyte-macrophage colony-stimulating factor in pulmonary homeostasis. *Science* 264: 713–716, 1994.
8. **Gordon S, Taylor PR.** Monocyte and macrophage heterogeneity. *Nat Rev Immunol* 5: 953–964, 2005.
9. **Gough NM, Gough J, Metcalf D, Kelso A, Grail D, Nicola NA, Burgess AW, Dunn AR.** Molecular cloninog of cDNA encoding a murine haematopoietic growth regulator, granulocyte-macrophage colony stimulating factor. *Nature* 309: 763–767, 1984.
10. **Halseth AE, Bracy DP, Wasserman DH.** Overexpression of hexokinase II increases insulinand exercise-stimulated muscle glucose uptake in vivo. *Am J Physiol Endocrinol Metab* 276: E70–E77, 1999.
11. **Herbelin A, Machavoine F, Dy M.** Potentiating effect of granulocyte-macrophage colony-stimulating factor on interleukin-1-induced thymocyte proliferation: evidence for an interleukin-2 and tumor necrosis factor-independent pathway. *Lymphokine Res* 9: 155–165, 1990.
12. **Huffman Reed JA, Rice WR, Zsengeller ZK, Wert SE, Dranoff G, Whitsett JA.** GM-CSF enhances lung growth and causes alveolar type II epithelial cell hyperplasia in transgenic mice. *Am J Physiol Lung Cell Mol Physiol* 273: L715–L725, 1997.
13. **Lang RA, Metcalf D, Cuthbertson RA, Lyons I, Stanley E, Kelso A, Kannourakis G, Williamson DJ, Klintworth GK, Gonda TJ, Dunn AR.** Transgenic mice expressing a hemopoietic growth factor gene (GM-CSF) develop accumulations of macrophages, blindness, and a fatal syndrome of tissue damage. *Cell* 51: 675–686, 1987.
14. **Lee JY, Muenzberg H, Reed JA, Berryman D, Gavrilova O, Villanueva EC, Louis GW, Leinninger GM, Bertuzzi S, Robinson GW, Seeley RJ, Myers MG, Hennighausen L.** Loss of cytokine-Stat5 signaling in the CNS and the pituitary gland alters energy balance and leads to obesity. *PLoS One* 3: e1639, 2008.
15. **LeVine AM, Reed JA, Kurak KE, Cianciolo E, Whitsett JA.** GM-CSF-deficient mice are susceptible to pulmonary group B streptococcal infection. *J Clin Invest* 103: 563–569, 1999.
16. **Lumeng CN, Bodzin JL, Saltiel AR.** Obesity induces a phenotypic switch in adipose tissue macrophage polarization. *J Clin Invest* 117: 175–184, 2007.
17. **Mantovani A, Sica A, Sozzani S, Allavena P, Vecchi A, Locati M.** The chemokine system in diverse forms of macrophage activation and polarization. *Trends Immunol* 25: 677–686, 2004.
18. **Metcalf D, Begley CG, Williamson DJ, Nice EC, De Lamarter J, Mermod JJ, Thatcher D, Schmidt A.** Hemopoietic responses in mice injected with purified recombinant murine GM-CSF. *Exp Hematol* 15: 1–9, 1987.
19. **O′Brien AD, Standiford TJ, Christensen PJ, Wilcoxen SE, Paine R, 3rd.** Chemotaxis of alveolar macrophages in response to signals derived from alveolar epithelial cells. *J Lab Clin Med* 131: 417–424, 1998.
20. **Odegaard JI, Ricardo-Gonzalez RR, Goforth MH, Morel CR, Subramanian V, Mukundan L, Eagle AR, Vats D, Brombacher F, Ferrante AW, Chawla A.** Macrophage-specific PPARgamma controls alternative activation and improves insulin resistance. *Nature* 447: 1116–1120, 2007.
21. **Paine R, 3rd Morris SB, Jin H, Wilcoxen SE, Phare SM, Moore BB, Coffey MJ, Toews GB.** Impaired functional activity of alveolar macrophages from GM-CSF-deficient mice. *Am J Physiol Lung Cell Mol Physiol* 281: L1210–L1218, 2001.
22. **Paine R, 3rd Preston AM, Wilcoxen S, Jin H, Siu BB, Morris SB, Reed JA, Ross G, Whitsett JA, Beck JM.** Granulocyte-macrophage colony-stimulating factor in the innate immune response to Pneumocystis carinii pneumonia in mice. *J Immunol* 164: 2602–2609, 2000.
23. **Ravussin E, Smith SR.** Increased fat intake, impaired fat oxidation, and failure of fat cell proliferation result in ectopic fat storage, insulin resistance, and type 2 diabetes mellitus. *Ann NY Acad Sci* 967: 363–378, 2002.
24. **Reed JA, Clegg DJ, Smith KB, Tolod-Richer EG, Matter EK, Picard LS, Seeley RJ.** GM-CSF action in the CNS decreases food intake and body weight. *J Clin Invest* 115: 3035–3044, 2005.
25. **Reed JA, Ikegami M, Cianciolo ER, Lu W, Cho PS, Hull W, Jobe AH, Whitsett JA.** Aerosolized GM-CSF ameliorates pulmonary alveolar proteinosis in GM-CSF-deficient mice. *Am J Physiol Lung Cell Mol Physiol* 276: L556–L563, 1999.
26. **Sandoval DA, Ping L, Neill RA, Gong B, Walsh K, Davis SN.** Brain region-dependent effects of dexamethasone on counterregulatory responses to hypoglycemia in conscious rats. *Am J Physiol Regul Integr Comp Physiol* 288: R413–R419, 2005.
27. **Seelentag WK, Mermod JJ, Montesano R, Vassalli P.** Additive effects of interleukin 1 and tumour necrosis factor-alpha on the accumulation of the three granulocyte and macrophage colony-stimulating factor mRNAs in human endothelial cells. *Embo J* 6: 2261–2265, 1987.
28. **Shoelson SE, Herrero L, Naaz A.** Obesity, inflammation, and insulin resistance. *Gastroenterology* 132: 2169–2180, 2007.
29. **Shoelson SE, Lee J, Goldfine AB.** Inflammation and insulin resistance. *J Clin Invest* 116: 1793–1801, 2006.
30. **Strissel KJ, Stancheva Z, Miyoshi H, Perfield JW, 2nd DeFuria J, Jick Z, Greenberg AS, Obin MS.** Adipocyte death, adipose tissue remodeling, and obesity complications. *Diabetes* 56: 2910–2918, 2007.
31. **Vlahos R, Bozinovski S, Hamilton JA, Anderson GP.** Therapeutic potential of treating chronic obstructive pulmonary disease (COPD) by neutralising granulocyte macrophage-colony stimulating factor (GM-CSF). *Pharmacol Ther* 112: 106–115, 2006.
32. **Wall JS, Steele R, De Bodo RC, Altszuler N.** Effect of insulin on utilization and production of circulating glucose. *Am J Physiol* 189: 43–50, 1957.

33. **Weisberg SP, Hunter D, Huber R, Lemieux J, Slaymaker S, Vaddi K, Charo I, Leibel RL, Ferrante AW Jr.** CCR2 modulates inflammatory and metabolic effects of high-fat feeding. *J Clin Invest* 116: 115–124, 2006.
34. **Weisberg SP, McCann D, Desai M, Rosenbaum M, Leibel RL, Ferrante AW Jr.** Obesity is associated with macrophage accumulation in adipose tissue. *J Clin Invest* 112: 1796–1808, 2003.
35. **Wognum AW, Westerman Y, Visser TP, Wagemaker G.** Distribution of receptors for granulocyte-macrophage colony-stimulating factor on immature CD34+ bone marrow cells, differentiating monomyeloid progenitors, and mature blood cell subsets. *Blood* 84: 764–774, 1994.
36. **Woods SC, Seeley RJ, Rushing PA, D'Alessio D, Tso P.** A controlled high-fat diet induces an obese syndrome in rats. *J Nutr* 133: 1081–1087, 2003.
37. **Xu H, Barnes GT, Yang Q, Tan G, Yang D, Chou CJ, Sole J, Nichols A, Ross JS, Tartaglia LA, Chen H.** Chronic inflammation in fat plays a crucial role in the development of obesity-related insulin resistance. *J Clin Invest* 112: 1821–1830, 2003.
38. **Yoshida M, Ikegami M, Reed JA, Chroneos ZC, Whitsett JA.** GM-CSF regulates protein and lipid catabolism by alveolar macrophages. *Am J Physiol Lung Cell Mol Physiol* 280: L379–L386, 2001.
39. **Zsengeller ZK, Reed JA, Bachurski CJ, LeVine AM, Forry-Schaudies S, Hirsch R, Whitsett JA.** Adenovirus-mediated granulocyte-macrophage colony-stimulating factor improves lung pathology of pulmonary alveolar proteinosis in granulocyte-macrophage colony-stimulating factor-deficient mice. *Hum Gene Ther* 9: 2101–2109, 1998.